THE JOURNAL OF BIOLOGICAL CHEMISTRY
Vol. 278, No. 7, Issue of February 14, pp. 5444–5454, 2003
Printed in U.S.A.

Identification of a New Murine Tumor Necrosis Factor Receptor Locus That Contains Two Novel Murine Receptors for Tumor Necrosis Factor-related Apoptosis-inducing Ligand (TRAIL)*

Received for publication, October 21, 2002, and in revised form, November 27, 2002
Published, JBC Papers in Press, December 3, 2002, DOI 10.1074/jbc.M210783200

Pascal Schneider‡, Dian Olson§, Aubry Tardivel‡, Beth Browning§, Alexey Lugovskoy§, DaHai Gong§, Max Dobles§, Sylvie Hertig‡, Kay Hofmann¶, Herman Van Vlijmen§, Yen-Ming Hsu§, Linda C. Burkly§, Jurg Tschopp‡, and Timothy S. Zheng§‖

From the §Departments of Exploratory Sciences, Structural Informatics, Protein Chemistry, and Transgenics, Biogen, Inc., Cambridge, Massachusetts 02142, the ‡Institute of Biochemistry, University of Lausanne, BIL Biomedical Research Center, Chemin des Boveresses 155, CH-1066, Epalinges, Switzerland, and ¶MEMOREC Stoffel GmbH, Stoeckheimer Weg 1, D50829 Koeln, Germany

Tumor necrosis factor (TNF) ligand and receptor superfamily members play critical roles in diverse developmental and pathological settings. In search for novel TNF superfamily members, we identified a murine chromosomal locus that contains three new TNF receptor-related genes. Sequence alignments suggest that the ligand binding regions of these murine TNF receptor homologues, mTNFRH1, -2 and -3, are most homologous to those of the tumor necrosis factor-related apoptosis-inducing ligand (TRAIL) receptors. By using a number of *in vitro* ligand-receptor binding assays, we demonstrate that mTNFRH1 and -2, but not mTNFRH3, bind murine TRAIL, suggesting that they are indeed TRAIL receptors. This notion is further supported by our demonstration that both mTNFRH1:Fc and mTNFRH2:Fc fusion proteins inhibited mTRAIL-induced apoptosis of Jurkat cells. Unlike the only other known murine TRAIL receptor mTRAILR2, however, neither mTNFRH2 nor mTNFRH3 has a cytoplasmic region containing the well characterized death domain motif. Coupled with our observation that overexpression of mTNFRH1 and -2 in 293T cells neither induces apoptosis nor triggers NFκB activation, we propose that the *mTnfrh1* and *mTnfrh2* genes encode the first described murine decoy receptors for TRAIL, and we renamed them *mDcTrailr1* and *-r2*, respectively. Interestingly, the overall sequence structures of mDcTRAILR1 and -R2 are quite distinct from those of the known human decoy TRAIL receptors, suggesting that the presence of TRAIL decoy receptors represents a more recent evolutionary event.

In many biological systems, cellular outcomes are often determined by environmental cues delivered through ligand and receptor interactions on the cell surface. One group of ligand/receptor pairings critical to this decision-making process is the tumor necrosis factor (TNF)[1] ligand and receptor superfamily (1). Upon ligand engagement, TNF receptors trigger intracellular signaling pathways that lead to cell proliferation, differentiation, or apoptosis. The pivotal roles of these TNF ligands and receptors across diverse biological areas are perhaps best illustrated by gene knockout studies demonstrating the essential involvement of the lymphotoxin pathway in lymphoorganogenesis (2, 3), the BAFF pathway in B-cell development (4), the RANKL pathway in osteoclastogenesis (5), and the EDA pathway in hair-follicle formation (6). The ability of many members of this family to regulate both innate and adaptive immunity also makes them attractive targets for therapeutic intervention of various immune disorders, as exemplified by the success of anti-TNF therapy in treating rheumatoid arthritis and Crohn's disease (7).

TNF receptor family members are characterized by the presence of cysteine-rich repeats (CRDs) in their extracellular domains (8, 9). A CRD typically contains two structural motifs, called modules, that are stabilized by disulfide bridges formed between the cysteine residues. The linear arrangement of modules creates a scaffold that supports the unusual elongated structures seen in all known crystal structures of TNFR family members. In contrast to the absolute conservation of CRDs, the signaling potentials of TNF receptors vary a great deal. Whereas most TNF receptors, such as TNFR1, CD40, and Fas, have cytoplasmic domains containing well characterized signaling motifs such as TRAF-binding sites and/or death domain (10, 11), others lack signaling capacity. These non-signaling receptors include soluble receptors OPG and DcR3, the GPI-anchored human TRAILR3, and human TRAILR4 that contains a defective signaling cytoplasmic tail. The biological function of these so-called "decoy receptors" is likely to antagonize the pairing between ligands and their signaling receptor counterparts, providing a critical mechanism for ligand desensitization (12–15).

* This work was supported in part by grants from the Swiss National Science Foundation (to P. S. and J. T.). The costs of publication of this article were defrayed in part by the payment of page charges. This article must therefore be hereby marked "*advertisement*" in accordance with 18 U.S.C. Section 1734 solely to indicate this fact.

The nucleotide sequence(s) reported in this paper has been submitted to the GenBank™/EBI Data Bank with accession number(s) AY165625, AY165626, AY165627, and AY165628.

‖ To whom correspondence should be addressed: Dept. of Exploratory Sciences, Biogen, Inc., 12 Cambridge Center, Cambridge, MA 02142. Tel.: 617-679-3348; Fax: 617-679-3208; E-mail: timothy_zheng@biogen.com.

[1] The abbreviations used are: TNF, tumor necrosis factor; TRAIL, tumor necrosis factor-related apoptosis-inducing ligand; CRDs, cysteine-rich domains; TM, transmembrane; GPI, glycosylphosphatidylinositol; PBS, phosphate-buffered saline; TNFR, TNF receptor; mTNFR, murine TNF receptor; PI-PLC, phosphatidylinositol-specific phospholipase C; DMEM, Dulbecco's modified Eagle's medium; FCS, fetal calf serum; RT, reverse transcriptase; ELISA, enzyme-linked immunosorbent assay; aa, amino acid; FACS, fluorescence-activated cell sorter; CHAPS, 3-[(3-cholamidopropyl)dimethylammonio]-1-propanesulfonic acid; GFP, green fluorescent protein; BWS, Beckwith-Wiedemann syndrome; 7-AAD, 7-aminoactinomycin D; TRAF, TNF receptor-associated factor.

Whereas many members of the TNF ligand superfamily demonstrate one-to-one pairing with their cognate receptors, others exhibit complex ligand/receptor cross-talks (8). In particular, the TNF ligand TRAIL has five receptors in human, at least based on *in vitro* binding assays (16, 17). Among the hTRAIL receptors, hTRAILR1 and -R2 each contain a death domain in the cytoplasmic region, and as a result hTRAIL can efficiently induce caspase-dependent apoptosis in cell lines expressing these receptors (18, 19). As mentioned before, hTRAILR3 and -R4 are both considered decoy receptors, but their *in vivo* function is not clear. The fifth TRAIL-binding TNF receptor is OPG, which also binds to RANKL (17). Whereas studies of OPG knockout mice have clearly demonstrated OPG as a decoy receptor for RANKL, the *in vivo* relevance of OPG to TRAIL biology remains to be established (17, 20). Interestingly, only one murine TRAIL receptor, mTRAILR2/mKiller, has been identified so far (21). Similar to hTRAILR1 and -R2, mTRAILR2 contains a death domain motif and induces apoptosis when overexpressed or engaged by TRAIL.

Known as the TNF receptor "signature," the uniquely spaced cysteine residues found in these receptors allows identification of potential new family members from unprocessed genomic sequences by bioinformatic means. In this study, we describe the identification through genome mining of three new TNFR family members closely clustered on mouse chromosome 7. All three genes, named *mTNFRH1*, *-2* and *-3*, encode proteins containing classic TNF receptor-like CRDs. We also demonstrate that, whereas mTNFRH3 remains an orphan receptor, mTNFRH1 and two splice variants of mTNFRH2 can specifically bind murine TRAIL, but not the closely related RANKL nor any other ligand we have tested. Both sequence analysis and transient overexpression studies, however, suggest that mTNFRH1 and -2 are not signaling TRAIL receptors but rather the previously unknown murine TRAIL "decoy" receptors. Given their low overall sequence homology to hTRAILR3 and hTRAILR4, we propose that mTNFRH1 and -2 belong to a new class of TRAIL decoy receptors and thus named them mDcTRAILR1 and -R2, respectively. The identification of these two murine TRAIL decoy receptors will likely facilitate our understanding of the complex biology underlying TRAIL ligand/receptor interactions through the generation of mice deficient in these receptors.

EXPERIMENTAL PROCEDURES

Reagents—Anti-FLAG M2 monoclonal antibody, M2-agarose, and Biot-M2 were purchased from Sigma. PI-PLC from *Bacillus thuringiensis* was purchased from ICN Biochemicals (Aurora, OH). hTRAIL, hRANKL, hEDA, hTRAILR1:Fc, hTRAILR2:Fc, hTRAILR3:Fc, hTRAILR4:Fc, hOPG, and hEDAR:Fc were from Apotech (www.apotech.com). muOPG:Fc was purchased from R & D Systems (www.rndsystems.com). Cell culture reagents were from Invitrogen.

Cell Lines—293T cells were grown in DMEM supplemented with 10% heat-inactivated fetal calf serum (FCS). Jurkat cells were maintained in RPMI + 10% FCS and HEK-293 cells in DMEM:F12 + 2% FCS. All media contained 10 μg/ml each penicillin and streptomycin. All the cell lines used for Northern analysis were purchased from ATCC and grown in recommended culture media.

Transient transfections in 293T cells for the production of soluble proteins in serum-free Opti-MEM and establishment of stable transfectants in HEK-293 cells were performed as described previously (22).

Identification and Cloning of mDcTRAILR-1, mDcTRAILR-2 and mTNFRH-3 cDNAs—The cDNA of mTNFRH1/mDcTRAILR1 was obtained from EST clones (GenBank™ accession numbers AI156311, AI747041, and BG077775). A full-length coding cDNA was generated from these clones by a PCR-based method and cloned into the PCR-3 mammalian expression vector (Invitrogen).

The full-length cDNA clone of mTNFRH3 was obtained by screening a mouse spleen phage cDNA library (Stratagene) using a partial cDNA probe amplified from the E14 ES cell line. The screening was performed according to recommended protocol from Stratagene and resulted in one cDNA clone from about 1×10^6 independent clones.

The cDNAs of both splicing variants of mTNFRH2/mDcTRAILR2 were obtained by RT-PCR using primer sequences designed on genomic sequences. Briefly, total RNA was isolated from NIH3T3 cells using TRIzol (Invitrogen) followed by first strand synthesis using Superscript II (Invitrogen). PCR was performed using the Touchdown protocol. The cDNA of mTRAILR2/mKiller was obtained similarly using RNA from the J1 ES cell line.

Expression Vector—The PCR-3 mammalian expression vectors encoding the various FLAG ligand and receptor:Fc fusion proteins were generated as described (22), using cDNA sequences encoding the following amino acid residues: mDcTRAILR1 (aa 1–158), mDcTRAILR2$_L$ (aa 1–171), mDcTRAILR2$_S$ (aa 1–180), mTNFRH3 (aa 1–162), muTRAILR2 (aa 1–177), muRANK (aa 1–200), muTRAIL (aa 120–291), and muRANKL (aa 157–316).

Northern Analysis—Tissue expression patterns were done using premade Northern blots from Ambion. For expression patterns in various murine cell lines, total RNA was isolated using TRIzol reagent (Invitrogen), and 20 μg of total RNA was loaded for each lane. Probes for each gene were generated using PCR amplification of the coding regions and labeled with [α-^{32}P]dCTP using Ready-To-Go DNA labeling beads (Amersham Biosciences). Blots were hybridized and washed in ExpressHyb solution (Clontech) according to the manufacturer's protocol.

Coimmunoprecipitation and ELISA—Receptors:Fc (~500 ng) mixed with FLAG ligands (200 ng) in 1 ml of PBS were incubated for 2 h at 4 °C on a wheel with 2.5 μl of protein A-Sepharose (Amersham Biosciences). Beads were harvested, loaded in empty mini-columns, washed 3× with 100 volumes of PBS, eluted with 15 μl of 0.1 M citrate NaOH, pH 2.7, neutralized, and analyzed by Western blotting with anti-FLAG M2 antibody. Membranes were subsequently reprobed with goat anti-human IgG antibodies.

The interaction between receptor:Fc and FLAG ligands by ELISA was performed as described previously (23). Briefly, ELISA plates were coated with mouse anti-human IgG and then sequentially incubated at 37 °C with receptor:Fc, FLAG ligands, biotinylated M2, and horseradish peroxidase-coupled streptavidin. The binding of receptor:Fc was also probed directly with a horseradish peroxidase-coupled rabbit anti-human IgG polyclonal antibody.

Phospholipase C Treatment—Parental HEK-293 cells (2×10^5) and stable transfectants expressing full-length mDcTRAILR1 or full-length mDcTRAILR2$_L$ were incubated for 1 h at 37 °C in 100 μl of DMEM + 10% FCS containing or not 0.05 unit of PI-PLC from *B. thuringiensis*. After transfer on ice, cells were washed and sequentially stained with 50 μl of FLAG-muTRAIL (100 ng/ml), 50 μl of biotinylated M2 (1:500), and 50 μl of phycoerythrin-coupled streptavidin (1:500), and submitted to FACS analysis.

Cytotoxicity Assay—For mTRAIL-induced Jurkat cell death, assays were performed as described (22). Briefly, the TRAIL-sensitive Jurkat cells were incubated for 16 h with the indicated amount of FLAG-hTRAIL or FLAG-mTRAIL in the presence of 2 μg/ml anti-FLAG M2 cross-linking antibody. In other experiments, cell death induced by a fixed dose of FLAG-mTRAIL (50 ng/ml) + M2 antibody (2 μg/ml) was inhibited with the indicated amount of mDcTRAILR1:Fc, mDcTRAILR2:Fc, or hTRAILR2:Fc. Cell viability was measured by the phenazine methosulfate/3-(4,5-dimethylthiazol-2-yl)-5-(3-carboxymethoxyphenyl)-2-(4-sulfophenyl)-2*H*-tetrazolium assay (Promega).

For 293T cell death induced by expression of various TNF receptor family members, both adherent and floating cells, were collected 24–48 h post-transfection and stained with annexin V and 7-AAD (Pharmingen) according to the manufacturer's recommended protocol. Transfected cells were identified as cells expressing GFP. Dead cells were quantified as the percentage of GFP-positive cells that were also positive for 7-AAD staining.

Caspase and NFκB Activity Assays—For caspase activity assay, 293T cells (90-mm dish) were transfected with 7 μg of indicated plasmids. Cells were washed and harvested 24 h post-transfection and lysed in 70 μl of lysis buffer (0.2% Nonidet P-40, 20 mM Tris-HCl, pH 7.4, 150 mM NaCl, 10% glycerol) for 10 min on ice. Caspase activity was determined by loading 20 μl (triplicate) of lysates in black 96-well plate followed by addition of 100 μl of DEVDase buffer (0.1% CHAPS, 2 mM $MgCl_2$, 5 mM of EGTA, 150 mM NaCl, 10 mM Tris-HCl, pH 7.4, + 21 μl of 0.1 M dithiothreitol + 15 μl of DEVD-AMC 5 mM in Me_2SO). Fluorescence was then measured (excitation 355 nm, emission 460 nm) at different time points, and 5-h time point values are shown.

For NFκB assay, 2×10^5 293T cells were plated in each well of 24-well plates overnight and then transfected with various amounts of the indicated TNF receptor expressing vectors in triplicate together with 40 ng of an NFκB luciferase reporter construct. Luciferase activity

was measured 24 h post-transfection using the LucLite luciferase reporter gene assay kit (PerkinElmer Life Sciences).

mTRAIL Binding Assay—293T cells were transfected with various TNF receptor family members using the Polyfect Tranfection (Qiagen) protocol. Briefly, cells were plated at 5×10^5 cells/well in 6-well plates for 24 h and then cotransfected with 500 ng of a GFP expression construct (AN050) and various concentrations of expression constructs containing the individual TNF receptor family members. After 24–48 h, cells were harvested and sequentially stained with FLAG-tagged mTRAIL, an anti-FLAG M2 monoclonal antibody (Sigma, 1:2000), and phycoerythrin-conjugated anti-murine IgG (Jackson ImmunoResearch, 1:200) each for 30 min at 4 °C. All cell samples were analyzed on the BD Biosciences FACSCalibur.

To detect the binding of mTRAIL expressed on the cell surface, 293T cells were transfected with either mock vector or full-length murine TRAIL using LipofectAMINE 2000 (Invitrogen) according to the recommended protocol. The cells were harvested 24 h later with 5 mM EDTA in PBS and incubated for 1 h at room temperature with the following murine receptor Fc fusion proteins diluted in FACS buffer: DcTRAILR2$_L$:Fc (10 μg/ml), BCMA:Fc (10 μg/ml), TRAILR2:Fc at (10 μg/ml), and DcTRAILR2$_S$:Fc (100 μl of tissue culture supernatant). After washing, the cells were incubated with phycoerythrin-labeled goat anti-human IgG:Fc (Jackson ImmunoResearch) at 1:200 dilution for 30 min at room temperature. After final washes, cells were resuspended in 1% paraformaldehyde/PBS and analyzed using the BD Biosciences FACSCalibur.

Homology Modeling and Visualization—Models of *mTRAIL* trimer (residues 125–291) complexed to a single subunit of *mTNFRH3* (residues 41–148), *mDcTRAILR1* (residues 52–160), and *mDcTRAILR2* (residues 62–170) were built based on the crystal structure of human TRAIL/DR5 (TRAILR2) complex (Protein Data Bank code 1D4V (24)) using the homology modeling module of the InsightII program (version 2000, Accelrys (25)). The alignment of the receptors used for modeling is shown in Fig. 2*A*. Multiple models generated for each complex were validated using ProsaII program (25), and the ones having lowest the z scores were selected for further analysis. The models were visualized in the MOLMOL program (26).

RESULTS

Identification of the Murine TNFRHs Locus on Chromosome 7F4—To identify potential new TNF receptor family members, we used a TNFR signature profile (Prf:TNFR_NGFR_2 at www.expasy.ch/cgi-bin/nicedoc.pl?PDOC00561) to search a data base generated by the Swiss Institute of Bioinformatics that predicts proteins from the public genomic data bases. Our initial screening resulted in one TNFR signature-containing hit from the mouse genomic BAC clone RP23-6I17 (GenBank™ accession number AC068006). By using RT-PCR, we were able to confirm that this TNF receptor-like gene was indeed expressed (data not shown). Subsequent determination of its genomic localization revealed a tight linkage to two potentially novel TNF receptor homologous genes, *Tnfrh1* and *-2*, predicted from the genomic sequencing effort on the distal region of the mouse chromosome 7, the murine syntenic region of the Beckwith-Wiedemann syndrome (BWS) region in human ((27) GenBank™ accession number of the full genomic locus, AJ276505). Because the TNF receptor-like gene we identified is located to the immediate 3′ of the predicted *Tnfrh1* and *-2* genes, we named the gene *Tnfrh3*. Based on the above information, we hypothesized that there exists a previously unknown TNF receptor cluster on the distal region of mouse chromosome 7. We then proceeded to obtain the full-length coding regions of all three *Tnfrh* genes (see below), and we identified several BAC clones (Resgen) containing the entire *Tnfrhs* locus. Upon extensive sequencing efforts, we concluded that, sandwiched between the *obph1* and *car1* genes, the three *mTnfrh* genes span roughly 100 kb with no other apparent intervening genes, based on analysis using GenScan (Fig. 1*A*). Because of our functional data (see below), we propose to rename the first two Tnfrh genes *mDcTrailr1* and *-r2*.

Cloning, Sequence Analysis, and Expression Pattern of mTNFRHs—Upon data base search, we found that a full-length cDNA sequence containing the predicted cDNA sequence for *mDcTrailr1* had been isolated previously and reported in a patent filing (international publication number, WO 98/43998). We then employed two different approaches to obtain the complete coding sequences for *mDcTrailr2* and *mTnfrh3*. For *mTnfrh3*, partial cDNA fragment amplified by RT-PCR from total RNA prepared from the mouse ES cell line E14 was used to probe a Stratagene mouse spleen cDNA phage library, resulting in the isolation of a single *mTnfrh3* full-length cDNA clone (GenBank™ accession number AY165628). For *mDcTrailr2*, the full coding region was obtained by a combination of computer-assisted exon prediction and PCR amplification from 1st strand DNA synthesized from NIH3T3 total RNA, which revealed the presence of two alternatively spliced *mDcTrailr2* variants (GenBank™ accession numbers AY165626 and AY165627) (Fig. 1*B*).

As expected, each mTNFRH contains a signal peptide sequence at the N terminus followed by TNFR-like cysteine-rich repeats, consistent with the typical type I membrane protein topology observed in most TNFR family members (Fig. 1*B*). The structures of their CRDs are remarkably similar, with three tandem A1/B2 domains in both mDcTRAILR1 and mDcTRAILR2, whereas mTNFRH3 has two A1/B2 followed by one A2/B2 domain (8) (Fig. 1*C*). The C-terminal portions of the mTNFRHs, however, are surprisingly divergent. Whereas mTNFRH3 contains a typical transmembrane domain (TM), the C terminus of mDcTRAILR1 instead exhibits structural features of a GPI anchor addition signal (Fig. 1*B*) (28). The two splice variants of mDcTRAILR2 also diverge in their C termini. The cDNA spanning exons 1–7 contains a stop codon within exon 6 and encodes a secreted soluble receptor (mDcTRAILR2$_S$), whereas the splice variant lacking exon 6 encodes a longer isoform (mDcTRAILR2$_L$) containing a TM region and a short intracellular domain. Finally, mDcTRAILR1 and -R2 are highly homologous with 71% identity at the amino acid level (Fig. 1*B*), indicating a recent gene duplication event at this locus.

We next examined the expression patterns of mTNFRHs in both mouse tissues and cell lines. Based on Northern blot analysis, the expression of *mTnfrh3* is primarily restricted to lymphoid tissues with a single ~3-kb message detected in both the thymus and spleen and at low but detectable levels in the lung (Fig. 2*A*). The lymphoid-specific expression pattern of *mTnfrh3* was largely confirmed in Northern analysis of a number of murine cell lines, with its expression detected almost exclusively in lymphoid cell lines, including both the T and B lineages. The only noticeable exception is Colon 26, a colorectal adenocarcinoma cell line that also expressed *mTnfrh3* (Fig. 2*B*). The analysis of expression patterns of *mDcTrailr1 and mDcTrailr2,* however, is complicated by the extremely high homology between these two genes. Although we could confirm by RT-PCR that both *mDcTrailr1* and *-2* are indeed expressed genes (data not shown), we were unable to distinguish their individual expression patterns by Northern analysis due to cross-hybridization of the probe to both mRNAs. Instead, the combined expression of *mDcTrailr1 and mDcTrailr2*, as determined by the presence of at least one of the mRNA species, could be detected at low levels in all the mouse tissues upon prolonged exposure (data not shown). In contrast, the levels of expression were considerably higher in murine cell lines, and various levels of combined expression can be detected in most of mouse lines we have tested so far without obvious patterns in the tissue/organ origins of the positive cell lines (Fig. 2*C*).

Murine TNFRH1/DcTRAILR1 and TNFRH2/DcTRAILR2 Bind Specifically to the TNF Ligand TRAIL—The CRDs of

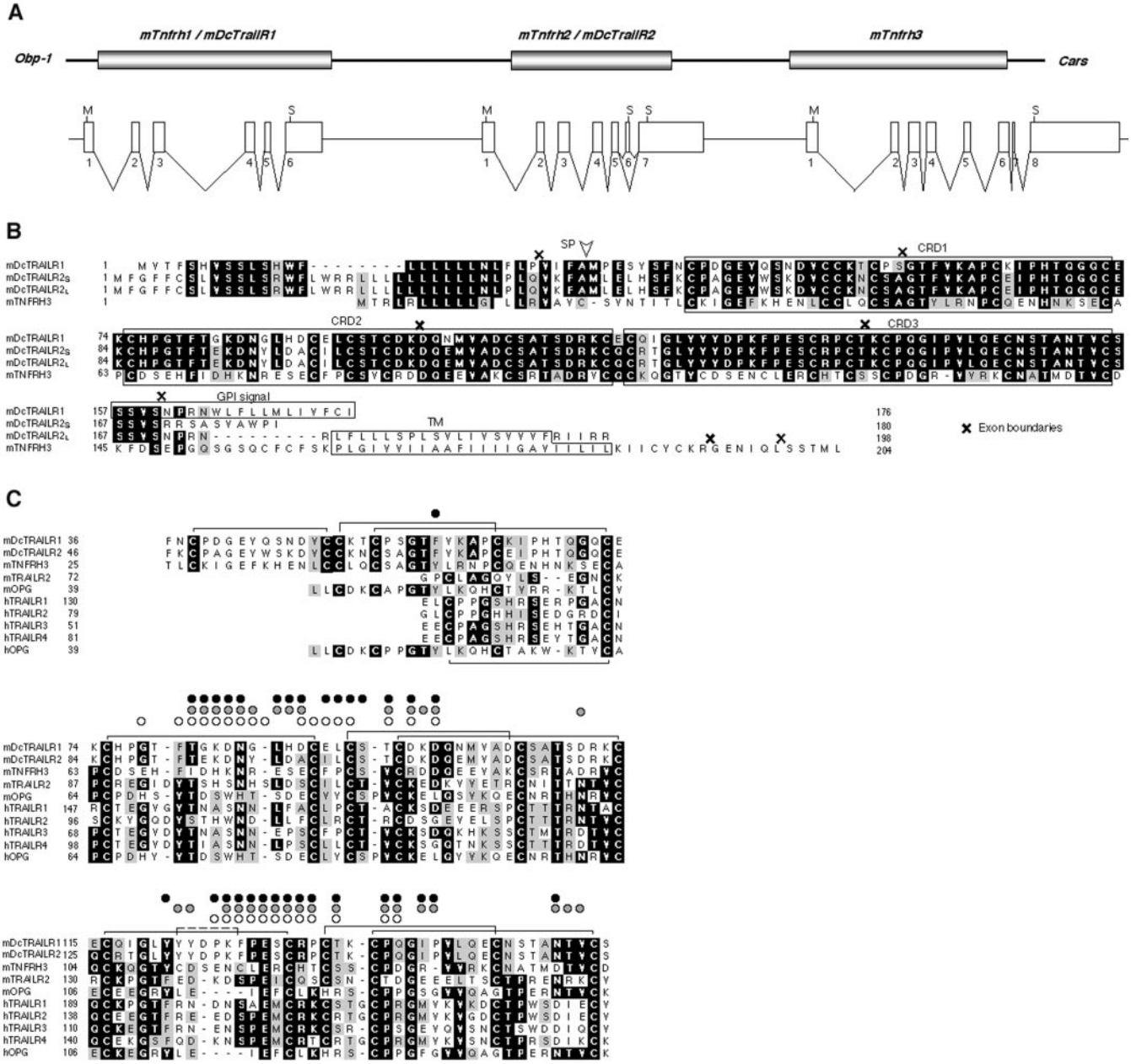

FIG. 1. *A*, genomic structure of the new murine TNF receptor locus on chromosome 7. Three TNF receptor family genes, *mTnfrh1/mDcTrailr1*, *mTnfrh2/mDcTrailr2*, and *mTnfrh3*, are clustered within 100 kb between Obph1 and Cars. The intron and intergenic sequences are shown at a 1:10 scale compared with exons. *M*, initiation codon for methionine; *S*, stop codon. There are two mRNA variants for *mTnfrh2/mDcTrailr2* due to alternative splicing of exon 6. *B*, alignment of the deduced amino acid sequences of mTNFRH1/mDcTRAILR1, mTNFRH2/mDcTRAILR1, and mTNFRH3 based on sequence homology. Identical residues are *dark-shaded*, and residues with similar properties are *light-shaded.* Exon-intron boundaries are indicated by *crosses above* the alignment. The *open arrows* indicates the predicted processing site of the signal peptide (*SP*). The cysteine-rich domains (CRD1, -2, and -3), the glycosylphosphatidylinositol addition signal (GPI signal), and the transmembrane domains (*TM*) are *boxed. C*, alignment of the CRD regions of mTNFRH1/mDcTRAILR1, mTNFRH2/mDcTRAILR1, mTNFRH3, and all other known TRAIL binding TNF receptors. The positions of disulfide bonds are marked by *squared brackets above* (or *below*) the sequences. The *dotted bracket* indicates the position of an additional disulfide bridge present in mTNFRH3 only. *Black*, *gray*, and *white dots above* the alignment indicate residues of muDcTRAILR1, muDcTRAILR2, and hTRAILR2, respectively, that interact with TRAIL (in the crystal structure of hTRAILR2 complexed with hTRAIL or in the model of muDcTRAILR1 and muDcTRAILR2 complexed with muTRAIL).

TNF receptors not only provide the overall structural scaffold but also determine their ligand binding specificity (8). In an attempt to "deorphanize" mTNFRHs, we performed sequence alignments of their CRD regions with those of the other known TNF receptors. Our analysis revealed significant homologies between mTNFRHs and TRAIL receptors, particularly in regions of the TRAIL receptors that are involved in binding to TRAIL (Fig. 1*C*), as suggested by the crystallographic studies of the hTRAIL-hTRAILR2 complex (24, 29, 30).

To examine experimentally whether these novel TNF receptors can indeed bind to the TNF ligand TRAIL, we first used an ELISA-based screening assay that has been optimized for the detection of interactions between TNF family ligands and receptors (22, 23). As shown in Fig. 3*A*, both mDcTRAILR1:Fc and mDcTRAILR2$_L$:Fc fusion proteins bound soluble mouse TRAIL. Interestingly, mDcTRAILR2 also bound soluble human TRAIL but to a lesser degree, whereas mDcTRAILR1 appeared species-specific and did not interact at all with human TRAIL. The interactions between mDcTRAILRs and soluble TRAIL appeared highly specific because no other TNF ligand, includ-

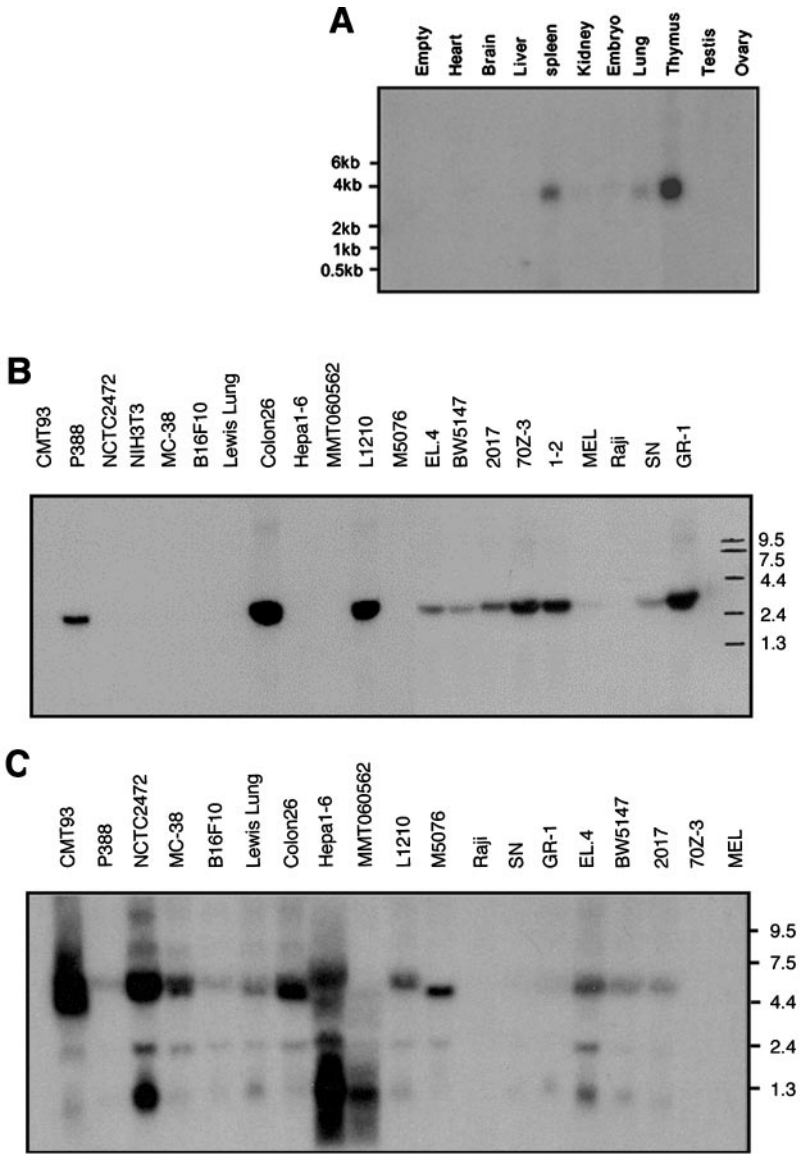

FIG. 2. *A*, tissue expression pattern of mTNFRH3 by Northern blot (Ambion). Relatively high expression of mTNFRH3 was detected in both thymus and spleen. Low but detectable expression was seen in the lung as well. *B*, expression pattern of mTNFRH3 in various murine cell lines by Northern blot. The expression of mTNFRH3 can be detected in all lymphoid cell lines as well as the colon carcinoma cell line Colon26. RNA from the human B-cell line Raji was loaded as a negative control. 20 μg of RNA was loaded for each cell line. *C*, combined expression pattern of mTNFRH1/mDcTRAILR1 and mTNFRH2/mDcTRAILR1 in murine cell lines by Northern blot. Several mRNA species can be detected in various cell lines. RNA from the human B-cell line Raji was loaded as a negative control. 20 μg of RNA was loaded for each cell line.

ing the closely related RANKL, bound to mDcTRAILR1:Fc and mDcTRAILR2$_L$:Fc in this assay (Fig. 3*A* and data not shown). Although the absolute binding affinities between these ligand/receptor pairings have not been measured, our observations are nonetheless suggestive of the possibility that mDcTRAILR1 and -R2 may compete effectively against muTRAILR2 for their common ligand TRAIL. Surprisingly, mTNFRH3:Fc did not bind to TRAIL, RANKL, or any other tested TNF ligand, despite its sequence homology to mDcTRAILR1 and -R2 and other TRAIL receptors (Fig. 3*A*). The ability of mDcTRAILR1 and -R2 to bind murine TRAIL was further examined by immunoprecipitation followed by Western blot. We found that, similar to hTRAILR2:Fc and mTRAILR2:Fc, both mDcTRAILR1:Fc and mDcTRAILR2$_L$:Fc efficiently precipitated FLAG-tagged murine TRAIL and again demonstrated the strict specificity of mDcTRAILR1 for murine but not human TRAIL (Fig. 3*B*). The ability of mDcTRAILR1 and -2 to bind TRAIL was further demonstrated using a biological assay in which both mDcTRAILR1:Fc and mDcTRALR2$_L$:Fc inhibited significantly mTRAIL-induced cytotoxicity in Jurkat cells (Fig. 3*C*).

We then confirmed the interactions between mTRAIL and mDcTRAILR1 and -R2 by using full-length mDcTRAILR1 and -R2 expressed on the cell surface (Fig. 3*D*). We found that mTRAIL readily bound to 293T cells expressing mTRAILR2, mDcTRAILR1, and mDcTRAILR2$_L$. The failure of soluble mTRAIL to bind 293T cells transfected with the mDcTRAILR2$_S$-expressing construct, as shown in Fig. 3*D*, is not surprising because mDcTRAILR2$_S$ lacks the transmembrane domain and does not express on the cell surface. To circumvent this problem, we tested the ability of mDcTRAILR2$_S$:Fc fusion protein to bind 293T cells expressing full-length mTRAIL on the surface. As shown in Fig. 3*E*, both mDcTRAILR2$_S$:Fc and mDcTRAILR2$_L$:Fc could bind surface mTRAIL. Based on these results, we conclude that mDcTRAILR1, mDcTRAILR2$_L$, and mDcTRAILR2$_S$ are indeed previously unknown murine TRAIL receptors.

Murine TNFRH-1/DcTRAILR-1 and TNFRH-2/DcTRAILR-2 Are Putative Murine Decoy TRAIL Receptors—Whereas both mDcTRAILR1 and mDcTRAILR2$_L$ appear to be surface receptors for TRAIL, sequence analysis also suggests that they anchor in the cytoplasmic membrane by different mechanisms. The C-terminal sequence of mDcTRAILR1 is a predicted glycosylphosphatidylinositol (GPI) anchor addition signal, whereas mDcTRAILR2$_L$ seems to contain a conventional transmembrane domain with an extremely short cytoplasmic domain. In both cases, the receptors do not seem to possess the ability, upon ligand engagement, to trigger the various intracellular signal transduction pathways involved in TRAIL-mediated cytotoxicity. In contrast, mDcTRAILR2$_S$ is a secreted soluble receptor.

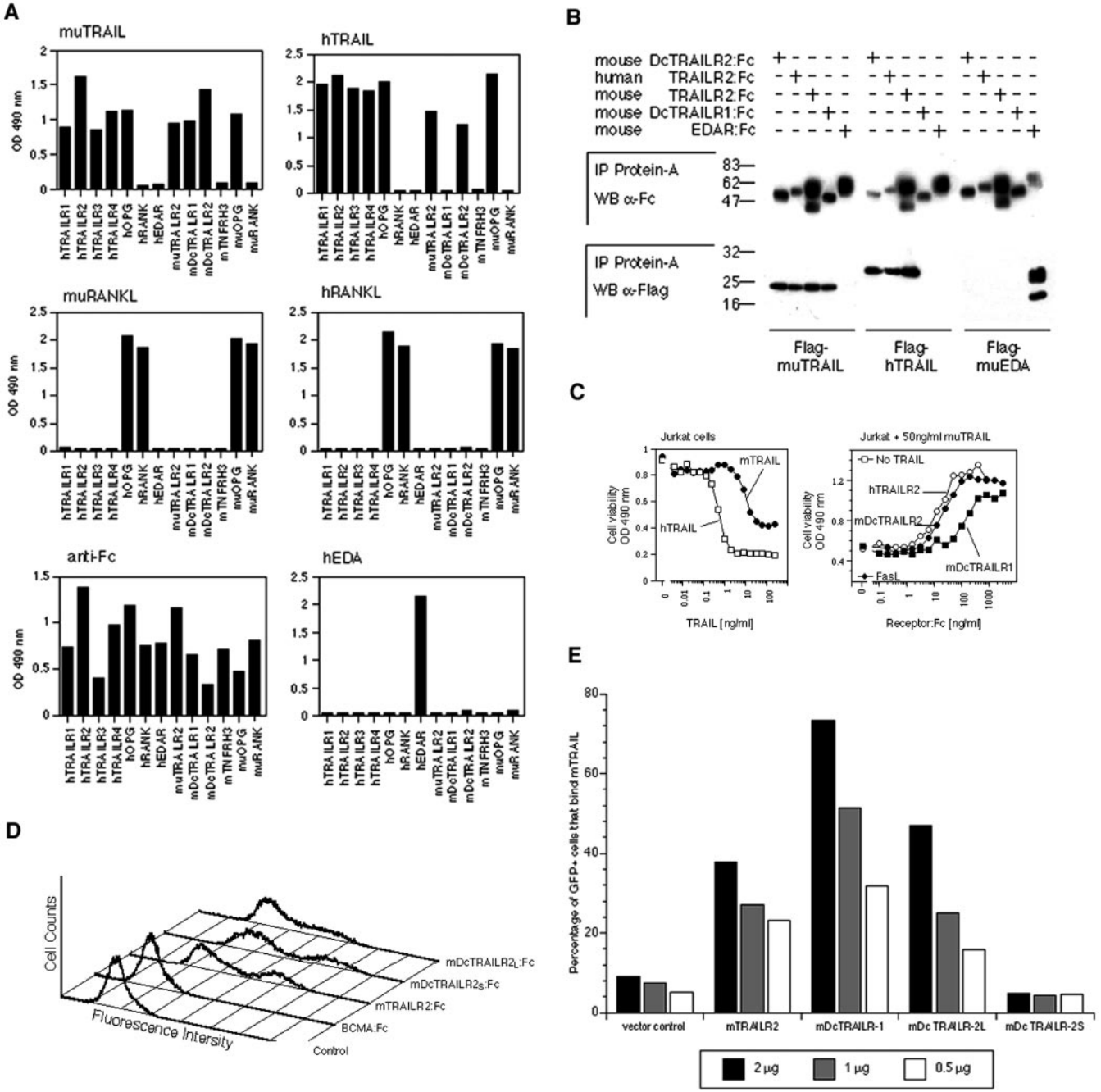

FIG. 3. **mDcTRAILR1 and -R2 are receptors for mTRAIL in both *in vitro* and cell-based assays.** *A*, receptor and species specificity of TRAIL and RANKL, as measured by ELISA. Receptor:Fc fusion proteins were allowed to interact with the indicated FLAG-tagged ligands at 37 °C. Efficient coating of the receptor:Fc fusion proteins was assessed with a goat anti-human antibody. The ectodysplasin-A–ectodysplasin-A receptor (EDA-EDAR) pair of ligand and receptor was used as a specificity control. *B*, receptor and species specificity of TRAIL, as measured by coimmunoprecipitation. FLAG-tagged hTRAIL, muTRAIL, and hEDA were incubated with the indicated receptor:Fc fusion proteins. Following immunoprecipitation (*IP*) with protein A-Sepharose, coimmunoprecipitated ligands were detected by anti-FLAG Western blot (*WB*) (*lower panels*). The blot was subsequently reprobed with an anti-human Ig antibody (*upper panels*). *C*, inhibition of mTRAIL-induced Jurkat cytotoxicity by mDcTRAILR1:Fc and R2:Fc. *Left panel*, titration of the cytotoxic activity of recombinant human and murine TRAIL on Jurkat cells. *Right panel*, Jurkat cell were treated for 16 h with a constant amount of muTRAIL (50 ng/ml) and in the presence of the indicating amounts of hTRAILR2:Fc, mDcTRAILR1:Fc, or mDcTRAILR2:Fc. Cell viability was measured by the phenazine methosulfate/3-(4,5-dimethylthiazol-2-yl)-5-(3-carboxymethoxyphenyl)-2-(4-sulfophenyl)-2*H*-tetrazolium assay. In this setting, untreated cells and cells treated with a lethal concentration of FasL gave $A_{490\ nm}$ of 1.4 and 0.27, respectively. *D*, FLAG-tagged soluble mTRAIL bound to 293T cells transiently transfected with full-length mTRAILR2, mDcTRAILR1, or mDcTRAILR2$_L$ but not mDcTRAILR2$_S$ which presumably is not expressed on the cell surface. All cells were also cotransfected with a GFP-expressing construct. The levels of binding, as measured by the percentage of GFP-positive cells that bind soluble mTRAIL by FACS analysis, correlated with the amounts of DNAs transfected. *E*, FACS analysis of binding of various receptor:Fc fusion proteins to mTRAIL expressed on the surface of 293T cells. 293T cells were transfected with a full-length mTRAIL-expressing construct and stained 24 h post-transfection with the following receptor:Fc proteins: BCMA:Fc, mDcTRAILR1:Fc, and mDcTRAILR2$_L$:Fc were all at 10 μg/ml and 100 μl of tissue culture supernatant from 293T cells transfected with an mDcTRAILR2$_S$:Fc-expressing construct.

To demonstrate formally that mDcTRAILR1, but not mDcTRAILR2$_L$, is a GPI-anchored receptor, we employed a well established method for assaying GPI anchorage of receptors by measuring the sensitivity of surface receptors to phosphatidylinositol-specific phospholipase C (PI-PLC) (31). As expected, surface expression of mDcTRAILR2$_L$, as determined by

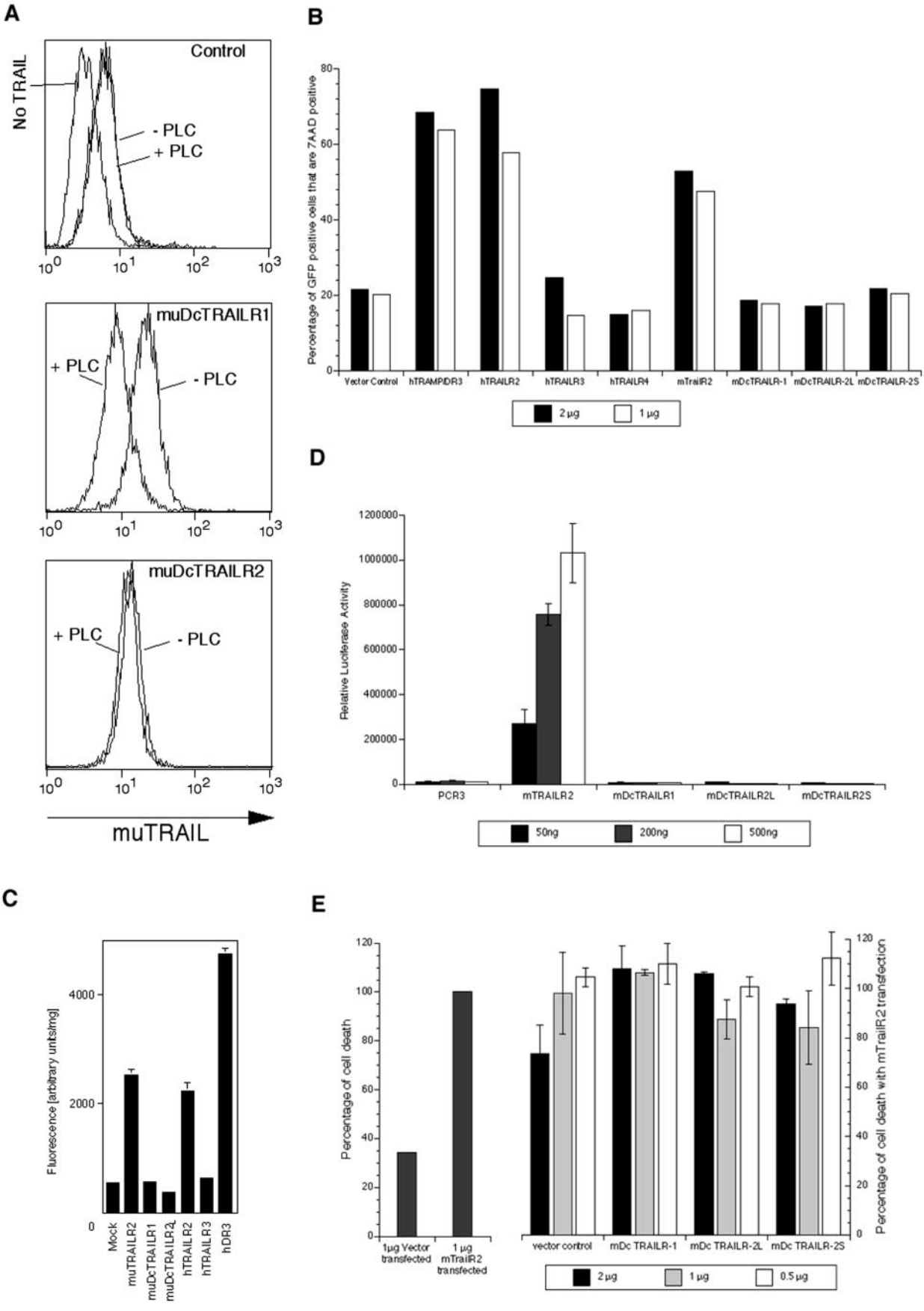

FIG. 4. *A*, PI-PLC sensitivity of mDcTRAILR1 and -R2. HEK-293 control cells and HEK-293 cells stably expressing mDcTRAILR1 or mDcTRAILR2 were treated with or without PI-PLC. Cells were subsequently stained with FLAG-tagged mTRAIL and analyzed by FACS. A control without TRAIL staining is shown in the *upper panel*. *B*, mDcTRAILR1, mDcTRAILR2$_L$, and mDcTRAILR2$_S$ do not induce apoptosis

mTRAIL staining, was not altered following PI-PLC treatment, indicating that mDcTRAILR2$_L$ anchors in the plasmic membrane through its conventional TM region (Fig. 4*A*). On the when other hand, an obvious decrease in mTRAIL staining could be detected in mDcTRAILR1-expressing 293 cells treated with PI-PLC (Fig. 4*A*), consistent with our hypothesis that mDcTRAILR1 is a GPI-linked surface TRAIL receptor.

Signaling TRAIL receptors hTRAILR1, hTRAILR2, and mTRAILR2 all contain the death domain motif in their cytoplasmic domains that is responsible for TRAIL-induced cytotoxicity, and the decoy receptors do not. Overexpression of these death domain-containing receptors can induce apoptosis in a number of cell lines such as 293 and NIH3T3, likely through self-oligomerization of the receptors. We therefore tested the effect of overexpression of mDcTRAILR1, mDcTRAILR2$_L$, and -R2$_S$, on 293T survival. As demonstrated in Fig. 4*B*, overexpression of death domain-containing receptors TRAMP/DR3, hTRAILR2, or mTRAILR2, but not the human decoy receptors hTRAILR3 and -4, resulted in significant cell death in 293T cell as measured by 7-AAD uptake. Transient transfection of mDcTRAILR1 and either the long or short form of mDcTRAILR2 did not have any noticeable effect on the survival of 293T cells, suggesting that mDcTRAILR1 and -R2 do not possess death-signaling capability. Consistent with this hypothesis, overexpression of mDcTRAILR1 and -R2 did not induce caspase activation that is characteristic of death receptor signaling, as demonstrated in Fig. 4*C*.

Many TNF receptor family members can also activate the NFκB pathway, through direct or indirect association with the TNF receptor-associated factor (TRAF) family members. Although mDcTRAILR1 and -R2 do not seem to possess the TRAF-binding motif according to sequence analysis, we nonetheless examined their ability to trigger indirectly NFκB activation (Fig. 4*D*). As reported previously (21), transient transfection of mTRAILR2 induced considerable NFκB activation in a dose-dependent manner as measured by cotransfection of an NFκB luciferase reporter construct. Overexpression of mDcTRAILR1 and both the long and short forms of mDcTRAILR2, however, failed to induce NFκB activity above that of the empty vector control level, again in agreement with the notion that both mTRAILR1 and -2 lack signaling capability and are likely murine TRAIL decoy receptors.

Previous studies (32) have suggested that decoy receptors could potentially inhibit ligand-induced cytotoxicity by directly competing for the ligand and/or disrupting the proper assembly of the signaling receptors. We have shown in Fig. 3*C* that apoptosis of Jurkat cells triggered by mTRAIL can indeed be efficiently blocked by both mDcTRAILR1:Fc and mDcTRALR2$_L$:Fc, supporting our hypothesis that mDcTRAILR1 and mDcTRAILR2 are likely decoy receptors that could function through ligand competition. To examine the latter possibility, we took advantage of the fact that receptor signaling induced by the overexpression of mTRAILR2 mimics that triggered by engagement of mTRAILR2 with TRAIL ligand. Our data clearly indicate that the presence of mDcTRAILR1 or mDcTRAILR2$_L$ has no apparent effect on 293T cell death induced by overexpression of mTRAILR2, suggesting that neither mDcTRAILR1 nor mDcTRAILR2$_L$ interferes with the proper assembly of mTRAILR2 that is required for transducing the apoptotic signaling (Fig. 4*D*).

DISCUSSION

In this study, we described the identification and characterization of a new TNF receptor locus where three TNF receptor-like genes, *Tnfrh1*, *-2* and *-3*, are located in tandem in the distal region of mouse chromosome 7. The close proximity of these three TNF receptor genes is not surprising as clusters of TNF family ligands and receptors can be found in many parts of the mammalian genome. For example, TNFα, LTα, and LTβ are all tightly clustered within the major histocompatibility region on chromosome 17 (mouse) and 6 (human). Similarly, two recently identified TNF ligands Tweak and April are also closely linked on human chromosome 17p13, whereas TL1A and CD30L are on 9q32-33. On the receptor side, TNF-RI, LTβ-R, and CD27 are located at 12p13 (human), whereas TNFR-RII, HVEM, CD30, and OX40 are clustered at 1p36 (human). Even more strikingly, all four known human receptors for TRAIL are found at 8p21-22. The presence of these clusters has led to the suggestion that the expanding TNF family has evolved from a limited number of ancestor molecules by means of gene duplication (1). Our identification of the *Tnfrhs* locus thus presents yet another example of TNF family clustering. Perhaps more interestingly, the *Tnfrh1*/*mDcTrailr1* and *Tnfrh2*/*mDcTrailr2* genes are extremely homologous with several stretches of genomic sequences that are nearly identical, indicative of a very recent duplicating event and providing by far the most convincing evidence supporting the gene duplication theory.

We also demonstrated experimentally that mTNFRH1 and -2, but not mTNFRH3, are receptors for TRAIL. Based on the sequence characteristics and a number of *in vitro* studies, we further propose that mTNFRH1 and -2 are in fact murine decoy receptors for mTRAIL, and we renamed them mDcTRAILR1 and mDcTRAILR2, respectively. Although whether these two murine TRAIL receptors function as decoy receptors *in vivo* remains to be formally established, several lines of evidence presented in this study, in particular their lack of both death signaling and NFκB activating capacity when overexpressed, are consistent with this hypothesis. Interestingly, there are considerable differences in the overall sequences between mDcTRAILR1 and -R2 and the previously known human decoy TRAIL receptors hTRAILR3 and -R4. Whereas the human receptors have the N1-A1-B2-A1-B2 cysteine module structure, both mDcTRAILR1 and mDcTRAILR2 have the A1-B2 domain instead of the N1 module. In addition, mDcTRAILR1 and -R2 do not possess either the membrane-proximal TAPE repeats that are characteristic of the huTRAILR3 or the truncated death domain present in huTRAILR4. These important differences suggest that, despite their apparent functional equivalence, the murine and human TRAIL decoy receptors likely have evolved independently.

overexpressed in 293T cells. 293T cells were cotransfected with either 2 or 1 μg of indicated TNF receptor expression vectors and 0.5 μg of GFP expression vector. Cells were harvested 48 h later and analyzed by FACS for cell death based on annexin V and 7-AAD staining. The data shown are representative of three separate experiments. *C*, transient transfection of mDcTRAILR1 and mDcTRAILR2$_L$ do not induce caspase activation in 293T cells. 293T cells were transfected with indicated TNF receptor expression vectors. Cells were harvested 24 h later, and cellular caspase activity was determined using the fluorogenic caspase substrate DEVD-AMC. The values shown are average of duplicate plates. *D*, mDcTRAILR1, mDcTRAILR2$_L$, and mDcTRAILR2$_S$ do not trigger NFκB activation when overexpressed in 293T cells. 293T cells were cotransfected with indicated amount of various TNF receptor expression vectors and 40 ng of an NFκB luciferase reporter construct. Cells were harvested 24 h later for luciferase activity assay, and the values shown are average of triplicate wells. *E*, cotransfection of mDcTRAILR1, mDcTRAILR2$_L$, and mDcTRAILR2$_S$ does not interfere with mTRAILR2-induced cell death in 293T cells. 293 cells were cotransfected with 1 μg of mTRAILR2 expression vector, 0.5 μg of GFP expression vector, and either with 2, 1, or 0.5 μg of indicated mDcTRAILRs. Cells were harvested 48 h later, and cell death was analyzed as described under "Experimental Procedures." The percentages of cell death are normalized against the absolute percentage of cell death induced by transfection of mTRAILR2 alone.

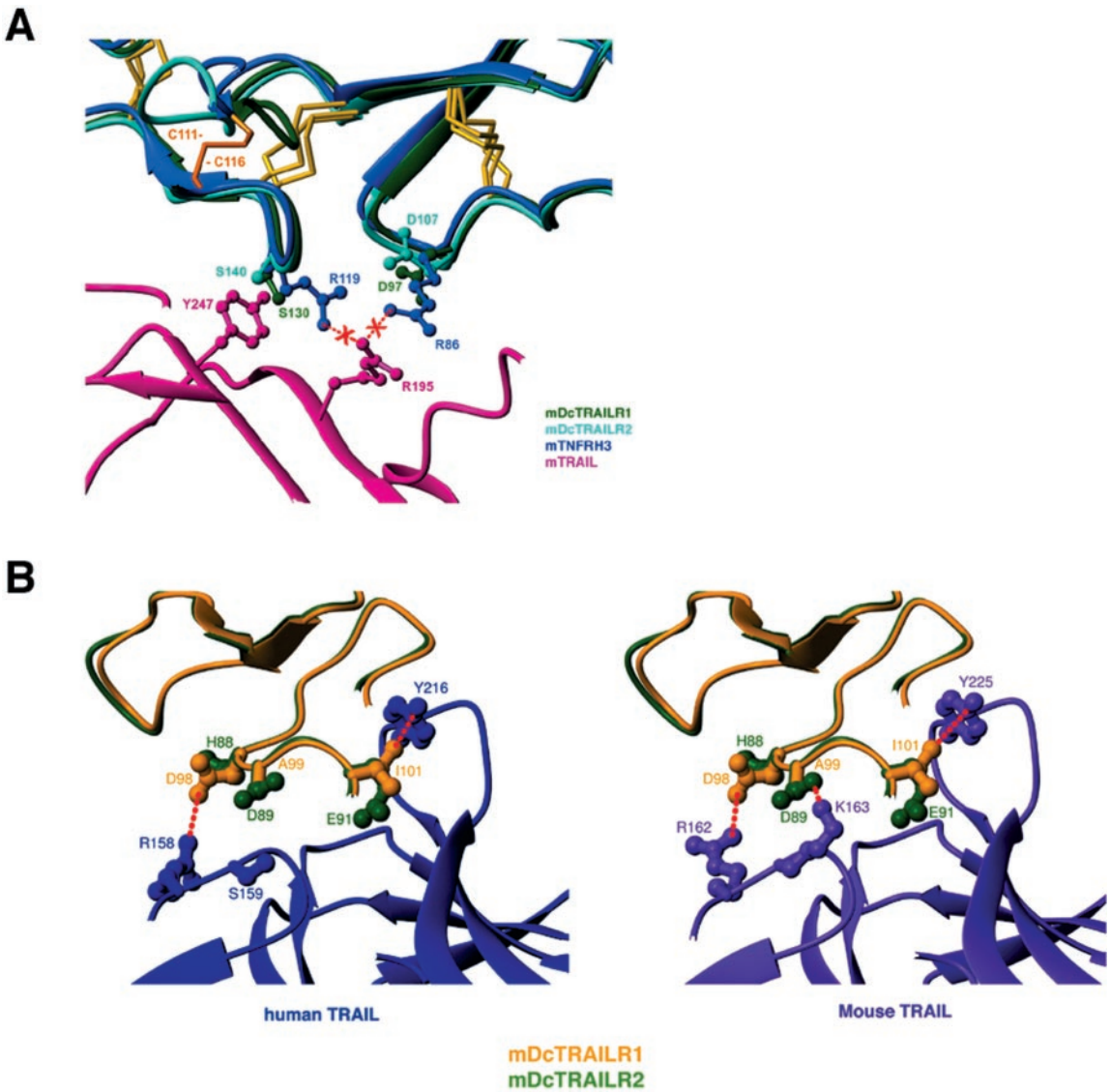

FIG. 5. *A*, portion of the modeled interface between mTRAIL (*pink*) and mDcTRAILR1 (*green*), mDcTRAILR2 (*cyan*), or mTNFRH-3 (*blue*). Intramolecular disulfide bonds are labeled *yellow* and *orange* for the extra disulfide bond in mTNFRH3. The hypothetic interface between mTRAIL and mTNFRH3 is likely destabilized due to the clustering of positively charged residues (Arg-86 and Arg-119 from mTNFRH3 and Arg-195 from mTRAIL). *B*, comparative modeling of simulated ligand/receptor interfaces between the CRD2 regions of mDcTRAILR1 or -R2 and human *versus* murine TRAIL. Potential interactions (both hydrophilic and hydrophobic) are marked in *red*. The strict species selectivity of mDcTRAILR1 for murine but not human TRAIL is likely due to an essential electrostatic interaction between Asp-89 of mDcTRAILR1 and Lys-163 of muTRAIL that is not present between mDcTRAILR1 and human TRAIL.

The divergence between mDcTRAILR1/R2 and hTRAILR3/R4 is also underscored by the potential differences in the mechanisms by which they inhibit TRAIL cytotoxicity. It has been reported previously (33) that, under physiological temperature, the affinities of hTRAILR3 and -R4 for hTRAIL are about 50–100-fold lower than those between hTRAIL and its cognate receptors hTRAILR1 and -R2. The observation suggests that the hTRAILR3 and -R4 would be very poor competitors for hTRAIL against hTRAILR1 and -R2, leading to the hypothesis that the human decoy TRAIL receptors might inhibit hTRAIL-induced cytotoxicity through some other mechanism(s), such as by disrupting the proper assembly of the trimeric cognate receptors (33). In our studies, however, we found that coexpression of mDcTRAILR1 or -R2 has no effect on cell death induced by mTRAILR2, arguing against such a scenario. It is therefore possible that the murine decoy receptors may function by a different mechanism than their human counterparts. Whether they can do so through direct competition for the ligand requires further investigation of the relative affinities of all murine TRAIL receptors for the TRAIL ligand.

The inability of mTNFRH3 to bind TRAIL is somewhat surprising given its sequence homology to mDcTRAILR1 and -R2. To understand the molecular basis of ligand selectivity exhibited by these receptors, we performed molecular modeling of the trimeric ligand/receptor interfaces between mTRAIL and various mTNFRHs based on the crystal structure of human TRAIL-TRAILR2 complex (Protein Data Bank code 1D4V) (24). As expected from the significant sequence homology in the CRD regions between hTRAILR2 and mDcTRAILR1 and -R2, the predicted interactions between mTRAIL and mDcTRAILR1 or -R2 mirror those between hTRAIL and hTRAILR2 to a large degree (Fig. 5*A* and data not shown).

Whereas the overall modeled structure of mTNFRH3 with mTRAIL is similar to that of mTRAIL with mDcTRAILR1 or -R2, we have identified two distinct features in the mTNFRH3 structure that may be responsible for its inability to bind

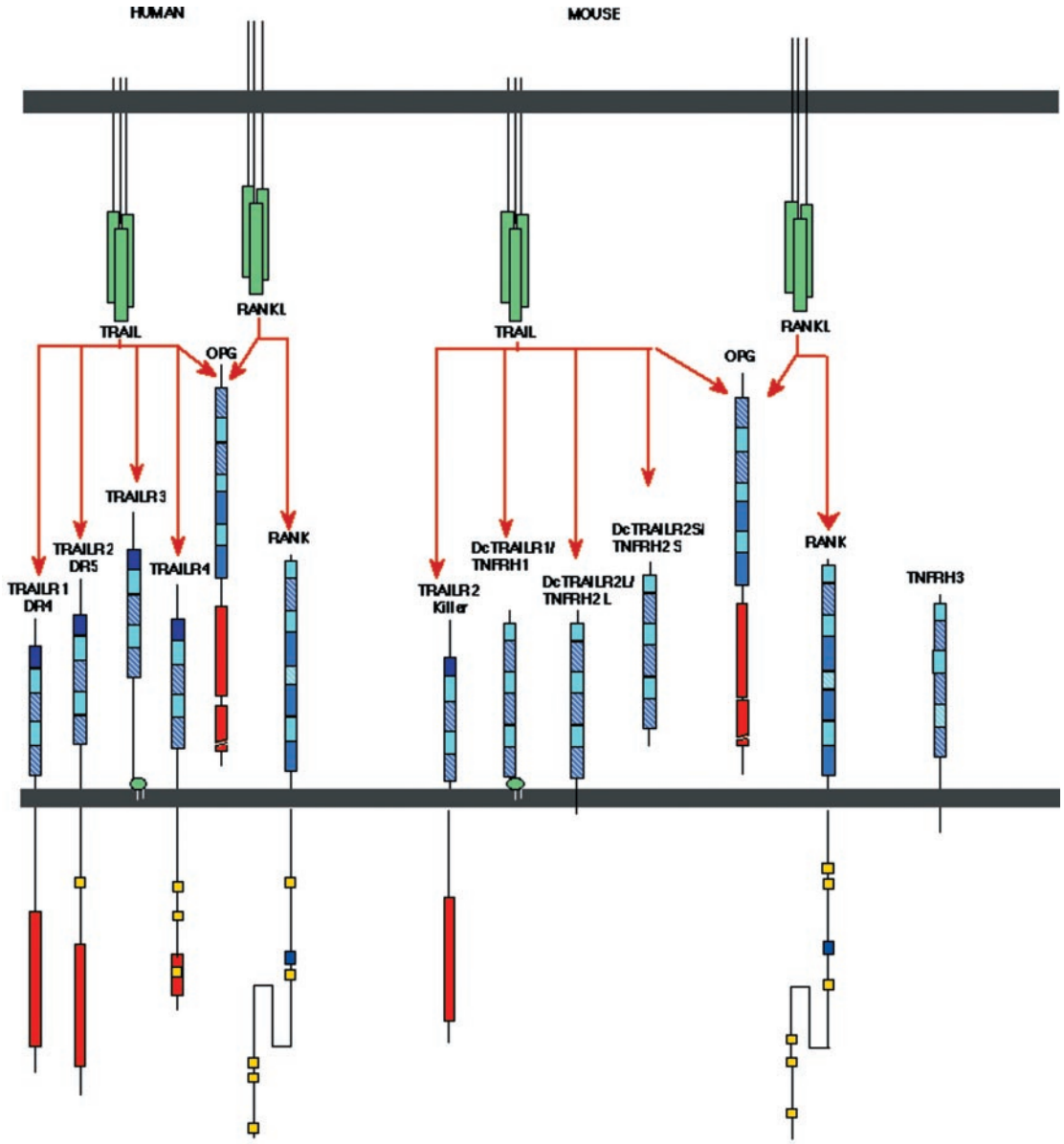

FIG. 6. **Summary of the interactions of TRAIL and RANKL with their cognate receptors in the human and murine systems.** Cysteine-rich modules in the extracellular region of the receptors are schematized according to Bodmer *et al.* (8). hTRAILR1, hTRAILR2, and mTRAILR2 contain an intracellular death domain (*large gray boxes*), and hTRAILR4 contains a truncated death domain. Consensus TRAF6-binding sequences are shown as *small gray boxes* (in hRANK and mRANK) and consensus binding sequences for other TRAFs are shown as *small open boxes*. hTRAILR3 and mDcTRAILR-1 are GPI-anchored receptors. The two splice variants of mdcTRAILR-2 (long and short) result in membrane-bound or secreted receptors, respectively. mTNFRH3 interacts neither with TRAIL nor with RANKL but is related in sequence to mdcTRAILR1 and -R2.

mTRAIL. Based on the modeling, cysteines 111 and 116 are positioned favorably to form a disulfide bond, resulting in the A1-B2-A2-B2 CRD module arrangement, rather than A1-B2-A1-B2 seen in mDcTRAILR1 or -R2. We also noticed that mTNFRH3 has two arginines in positions 86 and 119 that are not present in mDcTRAILR1 or -R2. When mapped on the hypothetical model of the mTRAIL-mTNFRH3 complex (Fig. 5*A*), these residues were found to be located proximally to Arg-195 of the mTRAIL, forming an unfavorable interaction between three positively charged residues. Both mDcTRAILR1 and -R2, however, can form a salt bridge with Arg-195 of mTRAIL via Asp-97 (mDcTRAILR1) or Asp-107 (mDcTRAILR2), stabilizing the interaction. The bulky nature of Arg-119 in mTNFRH3 also prevents its interaction with the side chain of Tyr-247 (mTRAIL) and instead promotes its reorientation toward Arg-86 (mTNFRH3) and Arg-195 (mTRAIL), resulting in the clustering of positive charges at the interface between mTNFRH3 and mTRAIL that makes the formation of a tight complex electrostatically unfavorable.

Our modeling further revealed possible structural basis for the strict species selectivity exhibited by mDcTRAILR1, which binds only mouse, but not human, TRAIL. Because mDcTRAILR2 is highly homologous to mDcTRAILR1 yet binds both human and mouse TRAIL, we closely examined the few residues involved in ligand binding that are different between mDcTRAILR1 and -R2, identifying a small cluster of such residues in the CRD2 regions of mDcTRAILR1 and -R2. As shown in Fig. 5*B*, it appears that the interface between mDcTRAILR1 and mTRAIL relies upon an important electrostatic interaction between Asp-89 of mDcTRAIL1 and the Lys-163 of mTRAIL. This salt bridge cannot occur with hTRAIL because it has the uncharged Ser-159 at this corresponding position. Although mDcTRAILR2 has Ala-99 at this position, which also precludes an electrostatic interaction with either Lys-163 in mTRAIL or Ser-159 in

hTRAIL, the interface between mDcTRAILR2 and either human or mouse TRAIL is stabilized by two additional interactions that do not exist between mDcTRAILR1 and the TRAIL ligand. The aspartic acid residue Asp-98 of the mDcTRAILR2, but not the corresponding His-88 in mDcTRAILR1, can form a salt bridge with Arg-158 of the hTRAIL and the corresponding Arg-162 in mTRAIL. Similarly, a favorable hydrophobic interaction exists between the Tyr-225 of human TRAIL (Tyr-216 of mouse TRAIL) and Ile-101 of mDcTRAILR2 but not the charged corresponding residue Glu-98 in mDcTRAILR1.

The locus linkage of mDcTRAIL1 and -R2 to the murine syntenic region of the human BWS locus is quite intriguing. Beckwith-Wiedemann syndrome is a congenital overgrowth syndrome whose pathogenesis has been linked to the abnormal imprint regulation of several candidate genes located at chromosome 11p15.5, a major imprinting cluster in the human genome (34). Given the role of TRAIL in tumor surveillance, it is tempting to speculate that the dysregulated expression of decoy receptors for TRAIL as a result of loss of imprint could potentially contribute to the failure in tumor suppression that is often associated with BWS. Because the two known human TRAIL decoy receptors are not located in the BWS region, the potential presence in the BWS region of human homologs of mDcTRAILR1 and -R2 that might be involved in the molecular pathology of BWS needs to be investigated.

The TRAIL pathway has been a subject of intense research in the past few years, largely due to the ability of TRAIL to preferentially kill tumor cell lines *in vitro* and *in vivo* (35–37). By using both TRAIL-deficient mice and a TRAIL-neutralizing antibody, more recent studies (38–40) have established that the TRAIL-mediated cytotoxicity pathway is critical for tumor surveillance by the immune system *in vivo*. Given the presence of both signaling and decoy receptors for TRAIL, it has been hypothesized that the ability of TRAIL to selectively target certain tumor cells is determined by the relative expression levels of these antagonizing receptors (14, 41). Repeated efforts, however, have failed to establish a clear link between TRAIL responsiveness and the expression pattern of various TRAIL receptors in many normal and tumor cells (39, 42). As a result, the *in vivo* function of the decoy TRAIL receptors and their relevance to the tumor-suppressing activity of TRAIL demonstrated in TRAIL-deficient mice remains unclear. In this study, we report the identification of putative decoy receptors for TRAIL in the mouse. Our discovery thus reveals that a comparably complex set of interactions between TRAIL ligand and its cognate as well as decoy receptors exists in both human and mouse (Fig. 6). The identification of these mDcTRAILR1 and -R2 will also make it possible to generate mice deficient in these decoy receptors, thus allowing definitive analysis of their possible *in vivo* contribution in modulating the sensitivity of different cell types to TRAIL.

REFERENCES

1. Locksley, R. M., Killeen, N., and Lenardo, M. J. (2001) *Cell* **104,** 487–501
2. Koni, P. A., Sacca, R., Lawton, P., Browning, J. L., Ruddle, N. H., and Flavell, R. A. (1997) *Immunity* **6,** 491–500
3. Rennert, P. D., Browning, J. L., Mebius, R., Mackay, F., and Hochman, P. S. (1996) *J. Exp. Med.* **184,** 1999–2006
4. Schiemann, B., Gommerman, J. L., Vora, K., Cachero, T. G., Shulga-Morskaya, S., Dobles, M., Frew, E., and Scott, M. L. (2001) *Science* **293,** 2111–2114
5. Kong, Y. Y., Yoshida, H., Sarosi, I., Tan, H. L., Timms, E., Capparelli, C., Morony, S., Oliveira-dos-Santos, A. J., Van, G., Itie, A., Khoo, W., Wakeham, A., Dunstan, C. R., Lacey, D. L., Mak, T. W., Boyle, W. J., and Penninger, J. M. (1999) *Nature* **397,** 315–323
6. Headon, D. J., and Overbeek, P. A. (1999) *Nat. Genet.* **22,** 370–374
7. Taylor, P. C. (2001) *Curr. Opin. Rheumatol.* **13,** 164–169
8. Bodmer, J. L., Schneider, P., and Tschopp, J. (2002) *Trends Biochem. Sci.* **27,** 19–26
9. Naismith, J. H., and Sprang, S. R. (1998) *Trends Biochem. Sci.* **23,** 74–79
10. Inoue, J., Ishida, T., Tsukamoto, N., Kobayashi, N., Naito, A., Azuma, S., and Yamamoto, T. (2000) *Exp. Cell Res.* **254,** 14–24
11. Hofmann, K. (1999) *Cell. Mol. Life Sci.* **55,** 1113–1128
12. Marsters, S. A., Sheridan, J. P., Pitti, R. M., Huang, A., Skubatch, M., Baldwin, D., Yuan, J., Gurney, A., Goddard, A. D., Godowski, P., and Ashkenazi, A. (1997) *Curr. Biol.* **7,** 1003–1006
13. Pitti, R. M., Marsters, S. A., Lawrence, D. A., Roy, M., Kischkel, F. C., Dowd, P., Huang, A., Donahue, C. J., Sherwood, S. W., Baldwin, D. T., Godowski, P. J., Wood, W. I., Gurney, A. L., Hillan, K. J., Cohen, R. L., Goddard, A. D., Botstein, D., and Ashkenazi, A. (1998) *Nature* **396,** 699–703
14. Sheridan, J. P., Marsters, S. A., Pitti, R. M., Gurney, A., Skubatch, M., Baldwin, D., Ramakrishnan, L., Gray, C. L., Baker, K., Wood, W. I., Goddard, A. D., Godowski, P., and Ashkenazi, A. (1997) *Science* **277,** 818–821
15. Simonet, W. S., Lacey, D. L., Dunstan, C. R., Kelley, M., Chang, M. S., Luthy, R., Nguyen, H. Q., Wooden, S., Bennett, L., Boone, T., Shimamoto, G., DeRose, M., Elliott, R., Colombero, A., Tan, H. L., Trail, G., Sullivan, J., Davy, E., Bucay, N., Renshaw-Gegg, L., Hughes, T. M., Hill, D., Pattison, W., Campbell, P., and Boyle, W. J. (1997) *Cell* **89,** 309–319
16. Griffith, T. S., and Lynch, D. H. (1998) *Curr. Opin. Immunol.* **10,** 559–563
17. Emery, J. G., McDonnell, P., Burke, M. B., Deen, K. C., Lyn, S., Silverman, C., Dul, E., Appelbaum, E. R., Eichman, C., DiPrinzio, R., Dodds, R. A., James, I. E., Rosenberg, M., Lee, J. C., and Young, P. R. (1998) *J. Biol. Chem.* **273,** 14363–14367
18. Pan, G., O'Rourke, K., Chinnaiyan, A. M., Gentz, R., Ebner, R., Ni, J., and Dixit, V. M. (1997) *Science* **276,** 111–113
19. Pan, G., Ni, J., Wei, Y. F., Yu, G., Gentz, R., and Dixit, V. M. (1997) *Science* **277,** 815–818
20. Bucay, N., Sarosi, I., Dunstan, C. R., Morony, S., Tarpley, J., Capparelli, C., Scully, S., Tan, H. L., Xu, W., Lacey, D. L., Boyle, W. J., and Simonet, W. S. (1998) *Genes Dev.* **12,** 1260–1268
21. Wu, G. S., Burns, T. F., Zhan, Y., Alnemri, E. S., and El-Deiry, W. S. (1999) *Cancer Res.* **59,** 2770–2775
22. Schneider, P. (2000) *Methods Enzymol.* **322,** 325–345
23. Thompson, J. S., Bixler, S. A., Qian, F., Vora, K., Scott, M. L., Cachero, T. G., Hession, C., Schneider, P., Sizing, I. D., Mullen, C., Strauch, K., Zafari, M., Benjamin, C. D., Tschopp, J., Browning, J. L., and Ambrose, C. (2001) *Science* **293,** 2108–2111
24. Mongkolsapaya, J., Grimes, J. M., Chen, N., Xu, X. N., Stuart, D. I., Jones, E. Y., and Screaton, G. R. (1999) *Nat. Struct. Biol.* **6,** 1048–1053
25. Šali, A. (1995) *MODELLER: Implementing 3D Protein Modeling*, Version 5.0, MC2 Molecular Simulations Inc., Burlington, MA
26. Koradi, R., Billeter, M., and Wuthrich, K. (1996) *J. Mol. Graphics* **14,** 51–55, 29–32
27. Engemann, S., Strodicke, M., Paulsen, M., Franck, O., Reinhardt, R., Lane, N., Reik, W., and Walter, J. (2000) *Hum. Mol. Genet.* **9,** 2691–2706
28. Udenfriend, S., and Kodukula, K. (1995) *Methods Enzymol.* **250,** 571–582
29. Hymowitz, S. G., Christinger, H. W., Fuh, G., Ultsch, M., O'Connell, M., Kelley, R. F., Ashkenazi, A., and de Vos, A. M. (1999) *Mol. Cell* **4,** 563–571
30. Cha, S. S., Sung, B. J., Kim, Y. A., Song, Y. L., Kim, H. J., Kim, S., Lee, M. S., and Oh, B. H. (2000) *J. Biol. Chem.* **275,** 31171–31177
31. Taguchi, R., Suzuki, K., Nakabayashi, T., and Ikezawa, H. (1984) *J. Biochem.* (*Tokyo*) **96,** 437–446
32. Chan, F. K., Chun, H. J., Zheng, L., Siegel, R. M., Bui, K. L., and Lenardo, M. J. (2000) *Science* **288,** 2351–2354
33. Truneh, A., Sharma, S., Silverman, C., Khandekar, S., Reddy, M. P., Deen, K. C., McLaughlin, M. M., Srinivasula, S. M., Livi, G. P., Marshall, L. A., Alnemri, E. S., Williams, W. V., and Doyle, M. L. (2000) *J. Biol. Chem.* **275,** 23319–23325
34. Maher, E. R., and Reik, W. (2000) *J. Clin. Invest.* **105,** 247–252
35. Ashkenazi, A., Pai, R. C., Fong, S., Leung, S., Lawrence, D. A., Marsters, S. A., Blackie, C., Chang, L., McMurtrey, A. E., Hebert, A., DeForge, L., Koumenis, I. L., Lewis, D., Harris, L., Bussiere, J., Koeppen, H., Shahrokh, Z., and Schwall, R. H. (1999) *J. Clin. Invest.* **104,** 155–162
36. Chinnaiyan, A. M., Prasad, U., Shankar, S., Hamstra, D. A., Shanaiah, M., Chenevert, T. L., Ross, B. D., and Rehemtulla, A. (2000) *Proc. Natl. Acad. Sci. U. S. A.* **97,** 1754–1759
37. Walczak, H., Miller, R. E., Ariail, K., Gliniak, B., Griffith, T. S., Kubin, M., Chin, W., Jones, J., Woodward, A., Le, T., Smith, C., Smolak, P., Goodwin, R. G., Rauch, C. T., Schuh, J. C., and Lynch, D. H. (1999) *Nat. Med.* **5,** 157–163
38. Takeda, K., Hayakawa, Y., Smyth, M. J., Kayagaki, N., Yamaguchi, N., Kakuta, S., Iwakura, Y., Yagita, H., and Okumura, K. (2001) *Nat. Med.* **7,** 94–100
39. Griffith, T. S., Wiley, S. R., Kubin, M. Z., Sedger, L. M., Maliszewski, C. R., and Fanger, N. A. (1999) *J. Exp. Med.* **189,** 1343–1354
40. Cretney, E., Takeda, K., Yagita, H., Glaccum, M., Peschon, J. J., and Smyth, M. J. (2002) *J. Immunol.* **168,** 1356–1361
41. Degli-Esposti, M. A., Dougall, W. C., Smolak, P. J., Waugh, J. Y., Smith, C. A., and Goodwin, R. G. (1997) *Immunity* **7,** 813–820
42. Griffith, T. S., Rauch, C. T., Smolak, P. J., Waugh, J. Y., Boiani, N., Lynch, D. H., Smith, C. A., Goodwin, R. G., and Kubin, M. Z. (1999) *J. Immunol.* **162,** 2597–2605